## ARTICLES

# Determination of the asymptotic $D$- to $S$-state ratio for $^3$He via $(\vec{d},^3\mathrm{He})$ reactions

Z. Ayer, H. J. Karwowski, B. Kozlowska,* and E. J. Ludwig
*Department of Physics and Astronomy, University of North Carolina at Chapel Hill, Chapel Hill, North Carolina 27599*
*and Triangle Universities Nuclear Laboratory, Durham, North Carolina 27708*
(Received 10 May 1995)

Angular distributions of the tensor analyzing powers $A_{yy}$ and $A_{zz}$ have been measured for the ground-state transition in the $^{93}$Nb$(\vec{d},^3$He$)^{92}$Zr reaction at $E_d=12$ MeV, and of $A_{zz}$ for the ground-state transitions in $^{63}$Cu$(\vec{d},^3$He$)^{62}$Ni at $E_d=8$ MeV and $^{89}$Y$(\vec{d},^3$He$)^{88}$Sr at $E_d=10.5$ MeV. The data are compared with predictions of full finite-range distorted-wave Born approximation (DWBA) calculations from which the asymptotic $D$- to $S$-state ratio, $\eta$, for $^3$He is extracted to be $-0.0386\pm0.0045\pm0.0012$. The difficulties with a choice of deuteron tensor optical potentials used in the DWBA calculations are discussed.

PACS number(s): 21.45.+v, 24.70.+s, 24.50.+g, 25.45.Hi

## I. INTRODUCTION

One manifestation of the tensor component of the nucleon-nucleon ($NN$) interaction in very light nuclei, such as $^3$He, is the presence of nonspherical components in the ground-state wave function. If the $^3$He nucleus is considered as a deuteron plus a proton, then in addition to the configuration where the relative orbital angular momentum ($L$) between the two is zero, the $S$ state, there also exists a configuration where $L=2$, the $D$ state. The presence of a $D$ state in light nuclei is exhibited in different ways. For example, in the deuteron the existence of a quadrupole moment ($Q_d$) is associated with the presence of a $D$ state. However, unlike the deuteron the three-nucleon systems (triton and $^3$He) do not possess a measurable quadrupole moment. In this case some other observable which is a measure of the $D$ state has to be determined. One such observable which can be determined reliably from experiment is the asymptotic $D$- to $S$-state ratio, $\eta$ [1]. The main motivation for determining $\eta$ for $^3$He is to study the $NN$ interaction and in particular the tensor force in the three-nucleon system which is responsible for ~50% of the binding and the presence of the $D$ state [2]. A practical application of this study stems from the considerable interest that exists in using a polarized $^3$He target as a polarized neutron target. The presence of a $D$ state in $^3$He dilutes the neutron polarization, since in this configuration the neutron spin is antiparallel to the $^3$He spin [3]. Our study of the $D$-state properties of $^3$He is part of a larger work investigating the three-nucleon system which has included a high-precision determination of $\eta$ for the triton [4].

Theoretical calculations of physical quantities for three-nucleon ($A=3$) systems have improved dramatically over the past few years. Exact Faddeev-type three-body calculations have been performed for the triton and $^3$He [5,6] and this has renewed interest in the determination of observables characterizing the $A=3$ system. The most precise measurements of $\eta$ have been done by analyzing transfer reactions induced by polarized deuterons. Calculations of tensor analyzing powers (TAPs) in $(\vec{d},^3$He) reactions are found to be sensitive to the $D$-state amplitude of the $d+p$ component in $^3$He [1].

In this paper TAP data measured in $(\vec{d},^3$He) transfer reactions are compared with distorted-wave Born approximation (DWBA) calculations and a best-fit value of $\eta$ is extracted. While previous $\eta$ determinations have also been made using this technique, in the present case the target nuclei and deuteron energies have been chosen so as to improve the reliability of the DWBA calculations used in the data analysis. This is discussed in greater detail in the following sections.

## II. BACKGROUND

### A. Previous determinations

In the $^3$He nucleus if $r$ is the separation of the proton from the deuteron center of mass, and $U_L(r)$ is the radial wave function of their relative motion with $L$ the relative orbital angular momentum between the two, then asymptotically $U_L(r)$ behaves as [1]

$$U_L(r)=N_L U_{NL}(r) \underset{r\to\infty}{\longrightarrow} \frac{N_L}{\alpha r} W_{-\xi,L+1/2}(2\alpha r).$$

Here $W_{-\xi,L+1/2}$ is a Whittaker function, and $\xi$ and $\alpha$ are the Coulomb parameter and wave number at the $^3$He$\to d+p$ vertex, respectively. The asymptotic $D/S$ state ratio, $\eta$, is defined as $\eta=N_2/N_0$.

Earlier determinations of the $D$-state amplitude in $^3$He focused on extraction of the parameter $D_2$ [1], which is approximately related to $\eta$ by $D_2\approx\eta/\alpha^2$, where

$$\alpha=(2\mu_{dp}B_{dp})^{1/2}$$

and $\mu_{dp}$ is the $d$-$p$ reduced mass while $B_{dp}$ is the $d$-$p$ binding energy in $^3$He. Measurements of TAPs in $(\vec{d},^3$He) reactions made in Refs. [7–9] were compared with DWBA calculations using the local energy approximation (LEA) [10]

*Present address: Physics Department, University of Silesia, Katowice, Poland.

 

which did not include a tensor potential in the entrance channel. The first finite-range calculations were made by Ioannides *et al.* [11] who showed differences with LEA calculations at backward angles. The tensor potential was first included in $(\vec{d},^3\mathrm{He})$ calculations using the LEA by Karban and Tostevin [12] who found that while the shape of the predicted TAPs did not change with the potential their magnitudes did. Entezami *et al.* [13] also included tensor potentials in an analysis using the LEA and confirmed the result of Karban and Tostevin. The most recent determination of $D_2$ was by Merz *et al.* [14] who performed a full finite-range DWBA analysis and also included the tensor potential in their calculations. DWBA analyses which included the tensor potential used a folding-model type parametrization for this potential as obtained by Keaton and Armstrong [15] with the magnitudes determined by fits to deuteron elastic-scattering data.

The more recent determinations of the $D$-state properties of $^3$He have concentrated on extracting the value of $\eta$. Different techniques have been used, though all involve the measurement of TAPs in deuteron-induced reactions. Vetterli *et al.* [16] reported an $\eta$ value of $-0.035\pm0.010$ obtained from the $^1\mathrm{H}(\vec{d},\gamma)^3\mathrm{He}$ radiative capture (RC) reaction at $E_d=19.8$ MeV. However, calculations for RC experiments are found to be relatively insensitive to the $D$-state properties of $^3$He and are strongly model dependent. Vuaridel *et al.* [17] used the technique of analytic continuation of tensor analyzing powers to the exchange pole in the $^4\mathrm{He}(\vec{d},^3\mathrm{He})^3\mathrm{H}$ reaction and obtained a value of $-0.035\pm0.006$. However, the treatment of systematic errors that arise in this procedure has been questioned by Londergan *et al.* [18]. Bhat *et al.* measured TAP's in the $^{31}\mathrm{P}(\vec{d},^3\mathrm{He})^{30}\mathrm{Si}$ [19] and $^{32}\mathrm{S}(\vec{d},^3\mathrm{He})^{31}\mathrm{P}$ [20] reactions at $E_d=16$ MeV and obtained $\eta$ values of $-0.042\pm0.007$ and $-0.046\pm0.005$, respectively. They used full finite-range DWBA calculations to analyze their data, but did not include a tensor potential in the deuteron channel.

Theoretical calculations of quantities characterizing the three-nucleon system such as $\eta$, rms charge radius, and electromagnetic form factors have been performed by the Los Alamos–Iowa [5] and Sendai [6] groups. Both groups, using different techniques, numerically solved the Faddeev equations for different sets of realistic nucleon-nucleon potentials, also including in some cases three-nucleon potentials. The resulting values of $\eta$, $\langle r^2\rangle$, etc. are found to have a linear dependence on the predicted binding energy and can be fit by a straight line (so-called Phillips line) [5]. At the physical binding energy for $^3$He (7.72 MeV) a value of $\eta=-0.043\pm0.001$ was obtained by the Los Alamos–Iowa group [5] and $-0.0414\pm0.0004$ by the Sendai group [6].

### B. Present determination

For the present work it was important to optimize the reliability of the finite-range DWBA calculations which are compared with data in order to extract a best-fit value of $\eta$. Ideally the incident deuteron energies should be below the Coulomb barrier. This is to reduce the sensitivity of the DWBA calculations to the choice of optical potentials. Owing to the small cross section at sub-barrier energies ($\ll$1 $\mu$b/sr) which render an analyzing-power measurement unfeasible, one is forced to make measurements at higher energies where count rates are adequate. The deuteron energies were therefore chosen as a compromise between expected statistical uncertainties and uncertainties arising from the choice of optical potentials in the DWBA calculations.

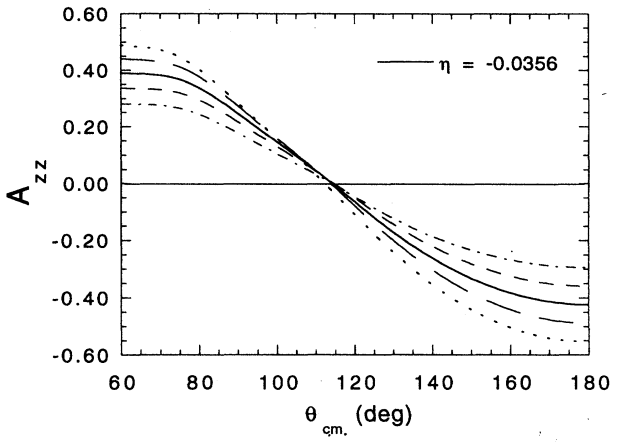


FIG. 1. Theoretical calculations of the tensor analyzing powers $A_{zz}$ for the $^{93}\mathrm{Nb}(\vec{d},^3\mathrm{He})^{92}\mathrm{Zr}$ reaction at $E_d=12$ MeV. The curves are obtained by varying the best-fit value of $\eta$ by $\pm15\%$ and $\pm30\%$. The long-dashed (short-dashed) curve corresponds to $\eta+0.15\eta$ ($\eta-0.15\eta$) and the dotted (dot-dashed) curve corresponds to $\eta+0.30\eta$ ($\eta-0.30\eta$).

TAPs were measured for the ground state (g.s.) transitions in the $^{93}\mathrm{Nb}(\vec{d},^3\mathrm{He})^{92}\mathrm{Zr}$ reaction at 12 MeV, the $^{63}\mathrm{Cu}(\vec{d},^3\mathrm{He})^{62}\mathrm{Ni}$ reaction at 8 MeV and the $^{89}\mathrm{Y}(\vec{d},^3\mathrm{He})^{88}\mathrm{Sr}$ reaction at 10.5 MeV. These reactions were chosen so as to involve unique $j$ transfers ($j^\pi=9/2^+$ for $^{93}$Nb, $3/2^-$ for $^{63}$Cu, and $1/2^-$ for $^{89}$Y) and have large spectroscopic factors for proton pickup. The former condition is chosen in order to avoid the ambiguity of summing multiple $l$-transfer spectroscopic amplitudes, while the latter condition enhances the reaction yield. In all the cases studied, the incident deuteron energies chosen are above the Coulomb barrier while the outgoing $^3$He particles are below the barrier. Also, our study was conducted with heavier targets where the finite-range DWBA analysis used to extract $\eta$ is generally more reliable than that for lighter targets [19,20].

The validity of the method applied in the present work is based on the fact that tensor analyzing powers calculated using DWBA scale directly with $\eta$ in reactions near the Coulomb barrier on heavy targets. Example of the scaling is shown in Fig. 1.

## III. EXPERIMENTAL PROCEDURE

The experiments were performed at Triangle Universities Nuclear Laboratory using polarized deuterons from an atomic-beam polarized ion source [21] and techniques described elsewhere [4]. The setting of transition units in the source yielded deuterons with tensor polarizations ($p_{zz}$) of $\pm0.70$. The quantization axis of the beam was defined by suitable setting of a Wien filter and the beam was injected into the FN tandem accelerator. After acceleration, the beam was momentum analyzed and sent to a 62 cm diameter scattering chamber. Typical beam currents on target were 0.5–1.0 $\mu$A.

The targets used were isotopically enriched, self-

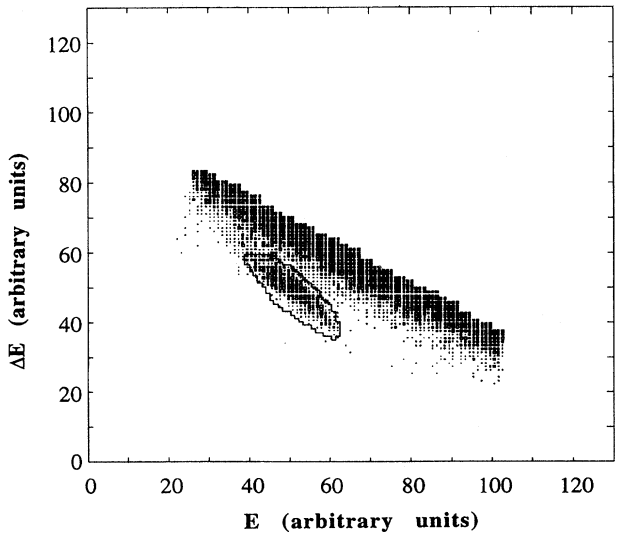


FIG. 2. Typical telescope spectrum obtained for the $^{63}$Cu($d$,$^3$He)$^{62}$Ni reaction. The $^3$He group is enclosed in a gate which is used to sort a $^3$He energy spectrum.

supporting foils which varied in thickness from 600 $\mu$g/cm$^2$ for $^{63}$Cu to about 2 mg/cm$^2$ for $^{89}$Y and $^{93}$Nb. Outgoing $^3$He particles were detected by three pairs of $\Delta E$-$E$ silicon surface-barrier detector telescopes arranged symmetrically on both sides of the incident beam. The thickness of the $\Delta E$ detectors varied from about 25 $\mu$m for the Cu target, to 50 and 75 $\mu$m for the Y and Nb targets depending on the scattering angles. For all targets the $E$ detectors were 300 $\mu$m thick. The telescopes subtended a solid angle of 6.63 msr and were set 15° apart. Measurements were made in 7.5° steps primarily at backward angles where the $D$-state effects on the TAP's are the greatest. A three-detector polarimeter located downstream from the target and utilizing the $^3$He($\vec{d}$,$p$)$^4$He reaction was used to monitor continuously the beam polarization [22].

Data were taken for three polarization states of the incident beam: an unpolarized state (state 1), a state with positive polarization (state 2), and a state with negative polarization (state 3). For the TAP data taken with the $^{93}$Nb target the states were switched on and off manually at intervals of approximately 45 minutes. However, for the $^{63}$Cu and $^{89}$Y data, an improved source control system allowed the state switching to be done under computer control over a period of less than 0.5 seconds. The advantage of this latter technique is that slow changes in experimental conditions such as beam position on target, target thickness, amplifier gain changes, affect the reaction yield for each spin state in the same way. Another improvement made to improve the quality of the $^{63}$Cu and $^{89}$Y data was to use a shorter resolving time between the $\Delta E$-$E$ coincidences (50 ns as opposed to 500 ns). This produced much cleaner $^3$He spectra and reduced the background due to $\alpha$ particles from the prevalent ($d$,$\alpha$) reaction. A typical $\Delta E$-$E$ telescope spectrum is shown in Fig. 2.

The symmetric arrangement of left and right detectors has the advantage that it compensates to first order for the effects of left-right shifts of beam position on target. The counts in the left and right telescopes were combined in order to determine $A_{yy}$ and $A_{zz}$. $A_{zz}$ was obtained from measurements made when the deuteron spin was oriented along the beam direction using the expression

$$A_{zz}=\frac{2(R-1)}{p_{zz}^{(2)}-Rp_{zz}^{(3)}},$$

where

$$R=\left[\frac{L^{(2)}+R^{(2)}}{L^{(3)}+R^{(3)}}\right]\text{NORM},$$

and NORM is the factor taking into account the dead-time corrections and the total charge accumulated for the two polarization states. The $L$ and $R$ refer to the counts in the left and right detectors, respectively, and the superscripts denote the polarization state. The expression for $A_{yy}$ is identical, except that $L$ and $R$ here are obtained with the spin quantization axis perpendicular to the scattering plane. Effects of the small vector polarization of the beam can be canceled for the $A_{yy}$ measurements by use of a symmetric detector setup.

Uncertainties shown with the data points consist of statistical errors arising from the primary ($d$,$^3$He) reaction and the beam polarization measurement. There is also a 3% uncertainty in the beam polarization values from the polarimeter calibration. This error is taken into account separately.

## IV. DATA ANALYSIS

Angular distributions of the TAPs $A_{yy}$ and $A_{zz}$ were measured for the ground state (g.s.) transition in the $^{93}$Nb($\vec{d}$,$^3$He)$^{92}$Zr reaction at 12 MeV. The TAP $A_{zz}$ was also measured for the g.s. transitions in $^{63}$Cu($\vec{d}$,$^3$He)$^{62}$Ni at 8 MeV and $^{89}$Y($\vec{d}$,$^3$He)$^{88}$Sr at 10.5 MeV. The data were analyzed with full finite-range DWBA calculations performed using a modified version of the computer code PTOLEMY [23]. For each reaction, three different sets of global deuteron optical potentials were used in the analysis. These sets were taken from Daehnick *et al.* [24], Lohr and Haeberli [25], and Perrin *et al.* [26], while for the $^3$He channel the global parameters of Becchetti and Greenlees [27] were used. The deuteron potential set of Lohr and Haeberli is based on an analysis of elastic cross-section and vector-analyzing-power (VAP) data taken on 22 nuclei in a mass range of $A=27$ and 208 and for deuteron energies between 9 and 13 MeV. The potential set of Perrin *et al.* is based on an analysis of cross-section and VAP data and also includes some TAP data taken for 10 nuclei with mass numbers varying from 12 to 208 and for a deuteron energy of 30 MeV. The global parameters from this potential set have been extrapolated for use at lower energies and have successfully described elastic-scattering data taken at energies as low as 9 MeV. The potential set of Daehnick *et al.* covers an energy range of 11.8 to 90 MeV and takes into account a much larger set of elastic cross-section and VAP data than the other potential sets considered here. All optical potential parameter sets for the deuteron channel include only central and spin-orbit terms.

The $^3$He wave function used in the calculations was generated in a Woods-Saxon well of radius 1.5 fm and diffuseness 0.5 fm. The depth of the well was adjusted so as to

TABLE I. Deuteron optical-model parameters yielding the best fits to elastic-scattering observables measured for $^{93}$Nb($\vec{d},d$)$^{93}$Nb at $E_d$=12 MeV. The notation and forms of the potentials are from Goddard and Haeberli (Ref. [28]). All depths are in MeV, and radii and diffuseness parameters in fm.

| Potential type | Depth | $r$ | $a$ |
|---|---|---|---|
| Real central ($V_R$) | 93.1 | 1.19 | 0.75 |
| Imaginary surface ($W_D$) | 13.6 | 1.30 | 0.78 |
| Real spin-orbit ($V_{SO}$) | 3.5 | 0.61 | 0.45 |
| Imaginary spin-orbit ($W_{SO}$) | 2.5 | 0.64 | 0.27 |
| Real tensor ($V_{TR}$) | −1.3 | 1.61 | 0.20 |
| Imaginary tensor ($W_{TR}$) | 1.1 | 1.58 | 0.56 |

reproduce the separation energy of the proton in $^3$He (separation-energy method). The wave function of the picked-up proton in the target nucleus was also generated in a Woods-Saxon well using the same method. Here, the radius and diffuseness parameters were 1.27 and 0.76 fm, respectively, and a real spin-orbit potential of depth 6.0 MeV was also included. It was found that the TAP's predicted by the DWBA calculations were not sensitive to the choice of well geometry.

The quantity used to judge the quality of the fits between the calculated and measured TAP's is the function $\chi^2$ defined by

$$\chi^2=\sum_1^N \left\{ \frac{A_{\rm exp}(\theta)-A_{\rm th}(\theta)}{\Delta A_{\rm exp}(\theta)} \right\}^2, \quad (1)$$

where $N$ is the number of data points, $A_{\rm exp}(\theta)$ is the quantity measured, $\Delta A_{\rm exp}(\theta)$ is its error, and $A_{\rm th}(\theta)$ is the theoretical value. For each set of deuteron potentials the best-fit value of $\eta$ was obtained by minimizing $\chi^2$ as a function of $\eta$.

In order to determine a reasonable deuteron optical model potential and to investigate the effects of including a deuteron-nucleus tensor potential, we measured the cross section, VAP and the TAPs $A_{yy}$ and $A_{zz}$ for $^{93}$Nb($\vec{d},d$)$^{93}$Nb at 12 MeV. The data were analyzed using the optical-model code DDTP [28]. The deuteron potential included complex central and spin-orbit terms, and a tensor potential of the $T_R$ type with a folding-model type parametrization [15]. Initial values for these parameters were taken from the best-fit values obtained by Goddard for $^{90}$Zr($\vec{d},d$)$^{90}$Zr at 12 MeV [28]. All parameters were then varied manually so as to obtain the best overall fit to all four observables. The quantity used to judge the quality of the fit is the function $\chi^2$ defined above. The parameters which yielded the minimum value of $\chi^2$ are listed in Table I. Since the code DDTP does not perform an automatic search of the parameter space to find the minimum value of $\chi^2$, the optical-model code HERMES [29] which includes such a search routine was used to verify that the parameters listed in Table I are indeed the values at which $\chi^2$ is a minimum. The data along with the best fits are shown in Fig. 3.

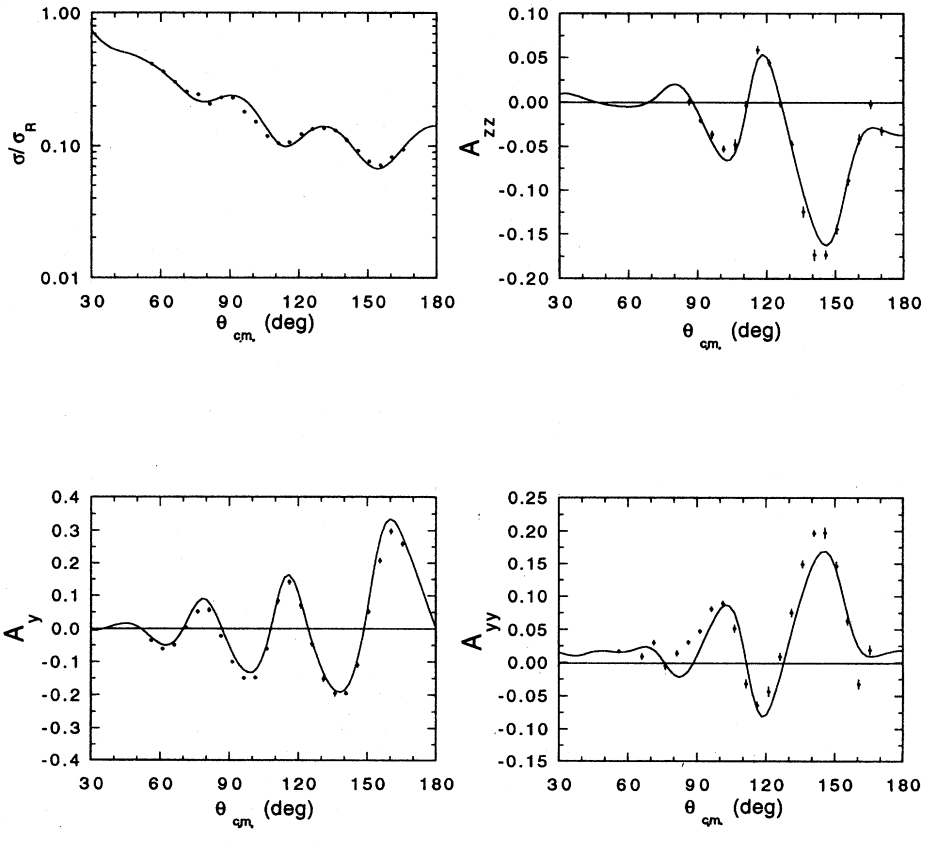


FIG. 3. Angular distributions of the cross section $\sigma$ divided by the Rutherford cross section $\sigma_R$, vector analyzing power $A_y$, and tensor analyzing powers $A_{yy}$ and $A_{zz}$ measured for $^{93}$Nb($\vec{d},d$)$^{93}$Nb at $E_d$=12 MeV. The curves are optical-model calculations which best fit the data.

TABLE II. Deuteron optical-model parameters for $^{93}$Nb taken from global analyses of deuteron elastic scattering. The notation of Daehnick *et al.* (Ref. [24]) has been used. All depths are in MeV, and radii and diffuseness parameters in fm.

| Potential set | $V_R$ | $r_0$ | $a_0$ | $W_D$ | $r_I$ | $a_I$ | $V_{LS}$ | $r_{LS}$ | $a_{LS}$ |
|---|---|---|---|---|---|---|---|---|---|
| Daehnick *et al.* [24] | 92.57 | 1.17 | 0.73 | 12.27 | 1.34 | 0.822 | 6.82 | 1.07 | 0.66 |
| Lohr and Haeberli [25] | 111.04 | 1.05 | 0.86 | 10.62 | 1.43 | 0.767 | 7.0 | 0.75 | 0.50 |
| Perrin *et al.* [26] | 85.31 | 1.13 | 0.80 | 12.0 | 1.32 | 0.812 | 5.2 | 0.85 | 0.475 |

## V. RESULTS AND DISCUSSION

Tensor analyzing powers $A_{zz}$ and $A_{yy}$ in the $^{93}$Nb($\vec{d}$,$^3$He)$^{92}$Zr reaction and $A_{zz}$ in the $^{63}$Cu($\vec{d}$,$^3$He)$^{62}$Ni and $^{89}$Y($\vec{d}$,$^3$He)$^{88}$Sr reactions were calculated using the three optical model (OM) global potential sets, DCV, LH, and Per. Listed in Table II are the deuteron potentials which were used for the $^{93}$Nb target. Other calculations for $^{93}$Nb were performed with the OM potential from Table I. Figure 4 shows a comparison of the four theoretical calculations together with the experimental $A_{zz}$ and $A_{yy}$ values for the $^{93}$Nb($\vec{d}$,$^3$He)$^{92}$Zr case. Each curve is the best fit to the data for a given potential set which is noted in the legend for the plot. Calculations performed with different OM sets give similar theoretical angular distributions of the tensor analyzing powers for every particular reaction which indicates that our extraction of $\eta$ is relatively insensitive to the deuteron optical potential. Figure 5 contains the results of $A_{zz}$ obtained for the $^{63}$Cu($\vec{d}$,$^3$He)$^{62}$Ni and $^{89}$Y($\vec{d}$,$^3$He)$^{88}$Sr reactions using only DCV OM potential. For the final determination of the $\eta$ value we took the best fit value obtained using the potential set of Daehnick *et al.* since this is the most recent and is therefore based on a larger data set than the potentials of Refs. [25] and [26].

Although the DWBA calculations are not very sensitive to the various sets of global OM potentials which contain the real, imaginary, and spin-orbit terms, the inclusion of the tensor potential term gives different results. When the poten-

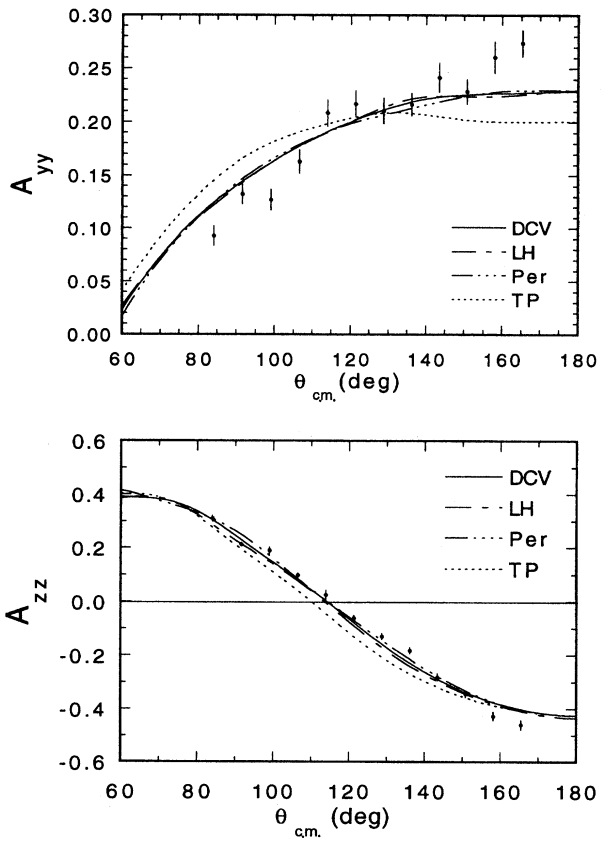


FIG. 4. Angular distributions of the tensor analyzing powers $A_{yy}$ (top) and $A_{zz}$ (bottom) measured in the $^{93}$Nb($\vec{d}$,$^3$He)$^{92}$Zr reaction at $E_d$=12 MeV. The curves are the best fits to the data obtained by varying $\eta$ using different potential sets. DCV, LH, and Per represent the potential sets of Refs. [24], [25], and [26], respectively. TP is the potential set from Table I.

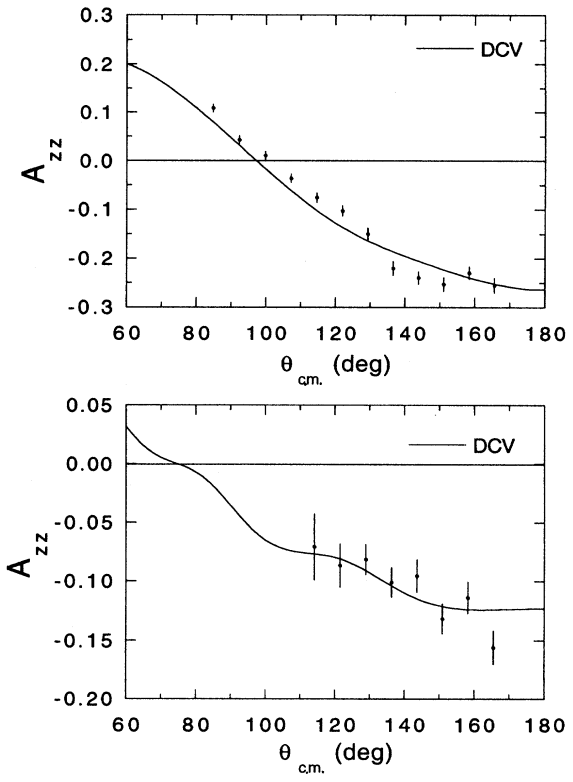


FIG. 5. Angular distributions of the tensor analyzing power $A_{zz}$ measured in the $^{63}$Cu($\vec{d}$,$^3$He)$^{62}$Ni reaction at $E_d$=8 MeV (top), and the $^{89}$Y($\vec{d}$,$^3$He)$^{88}$Sr reaction at $E_d$=10.5 MeV (bottom). The curves are the best fits to the data using the DCV OM potential.

tial set obtained from our fits to elastic-scattering observables is used in the DWBA calculations for the $^{93}$Nb($\vec{d}$,$^3$He)$^{92}$Zr reaction we see some marked differences in the resulting calculations compared with the global potentials (see Fig. 4). For the $A_{yy}$ data, the calculation does not describe the shape of the data. For the $A_{zz}$ data, the zero crossover in $A_{zz}$ is shifted towards forward angles by about 6 degrees, and here again the fit is poor. The inclusion of the tensor term in the optical-model potential appears to be responsible for this shift. Attempts to improve the fit to the reaction data by varying the magnitudes of the real and imaginary parts of this potential were not successful. One possible explanation for this lack of success is that the shape of the $T_R$ potential is not well established by fits to TAPs in deuteron elastic scattering. The form commonly used at sub-Coulomb energies which was employed in the present work is that of the standard folding model.

Similar difficulties in employing tensor potentials obtained from elastic scattering in calculations of reactions both above and below the Coulomb barrier were reported. Frick *et al.* [30] have shown in the case of $^{16}$O($\vec{d}$,$d$)$^{16}$O at $E_d$=20 MeV, that if the imaginary part of the tensor potential is kept fixed and the shape of the real part is varied, then predictions for the TAP $T_{21}(\theta)$ are found to be nearly identical. Frick *et al.* concluded that the poor knowledge of the tensor potential is a problem for the quantitative analysis of transfer reactions with tensor-polarized deuterons. This conclusion is borne out by our analysis of TAP for the $^{93}$Nb($\vec{d}$,$^3$He)$^{92}$Zr reaction which shows that the reaction observables appear best fit when the tensor potential is set to zero.

Even at sub-Coulomb energies the tensor potential is rather poorly known. In previous analyses [31–33], the magnitudes of the real and imaginary depths of this potential that have to be used in order to describe elastic-scattering data have varied between zero and the full values obtained by the folding model of Keaton and Armstrong [15]. In our analysis of TAP in ($d$,$t$) reactions at sub-Coulomb energies we used a model of Santos *et al.* [34] to determine the depths of the tensor potential [4].

There are also alternatives to the use of any tensor potentials in fits to elastic scattering TAP observables. Effects of coupling on TAP data in elastic scattering similar to those caused by the introduction of the folding-model tensor potential were discussed by Tostevin [35]. He showed that in the case of $^{208}$Pb, sub-Coulomb deuteron elastic-scattering data could be described well if coupling to specific ($\vec{d}$,$p$) channels is taken into account. We are not aware of this type of analysis for reactions at energies above the Coulomb barrier.

In view of contradictory conclusions concerning the role of more sophisticated potentials we assume in this work that cross-section and analyzing-power data in deuteron elastic scattering can be described adequately by the use of global potentials. These potentials describe transfer reaction data well and have been employed in most analyses of deuteron-induced reactions above the Coulomb barrier [19,20,36].

We have therefore extracted separate values of $\eta$ from each of the four angular distributions using the global potential sets of Daehnick *et al.* [24] in the deuteron channel and the global parameters of Becchetti and Greenlees [27] in the $^3$He channel. The values of $\eta$ were extracted by minimizing the $\chi^2$ parameter [Eq. (1)] between calculated and measured TAP's for different values of the asymptotic $D$-state amplitudes. The error in $\eta$, $\Delta\eta$, was taken to be the difference in the value of $\eta$ where $\chi^2$ is a minimum and the value of $\eta$ where $\chi^2$ is twice its minimum value. The extracted best-fit values of $\eta$ together with their statistical uncertainties, $\Delta\eta$, minimum $\chi^2$ per degree of freedom, $\chi^2/N$, and the number of points in the angular distributions are summarized in Table III.

The values listed for $\chi^2/N$ are based on the uncertainties in the individual data points. Since these values for three out of four measurements are significantly larger than 1 we assumed that there is either an unknown systematic error in the experimental data points or inadequate theoretical description of the present data or both. In order to account for all these effects which may have affected the measurements and be a source of an unknown uncertainty we followed the procedure described by Rosenfeld [37] and we multiplied our experimental errors by a scale factor $S=[\chi^2/N]^{1/2}$. As a result of this rather conservative approach the $\chi^2/N$ values became equal to 1.0 and the weighted average errors scaled up by the same factor $S$. The $S\Delta\eta$ errors are listed in the last column of Table III and are further used in calculating weighted average $\eta_{^3\mathrm{He}}$ and its error $\Delta\eta_{^3\mathrm{He}}$.

Our measurements of $\eta$ for different nuclei are consistent with each other which indicates that they are independent of nuclear structure effects. To obtain a final value of $\eta_{^3\mathrm{He}}$ we computed a weighted average of the four values listed in Table III, using the inverse square of each error $S\Delta\eta$ as a weighting factor. We obtain an $\eta_{^3\mathrm{He}}$ value of $-0.0386 \pm 0.0045$. There is also a systematic uncertainty of 3% in the beam polarization. We thus obtain a final $\eta_{^3\mathrm{He}}$ value of $-0.0386 \pm 0.0045 \pm 0.0012$.

## VI. SUMMARY AND CONCLUSIONS

From comparison of the TAP's measured in the $^{93}$Nb($\vec{d}$,$^3$He)$^{92}$Zr $^{63}$Cu($\vec{d}$,$^3$He)$^{62}$Ni, and $^{89}$Y($\vec{d}$,$^3$He)$^{88}$Sr reactions with full finite-range DWBA calculations, we extracted four independent values of $\eta$ for $^3$He. These values were

TABLE III. Values of $\eta \pm \Delta\eta$ extracted from the TAP data measured in ($\vec{d}$,$^3$He) reactions.

| Reaction | $E_d$ [MeV] | TAP | $\eta$ | $\chi^2/N$ | No. of pts | $\Delta\eta$ | $S\Delta\eta$ |
|---|---|---|---|---|---|---|---|
| $^{93}$Nb($\vec{d}$,$^3$He)$^{92}$Zr | 12.0 | $A_{zz}$ | −0.0356 | 6.0 | 12 | ±0.0047 | ±0.0115 |
| $^{93}$Nb($\vec{d}$,$^3$He)$^{92}$Zr | 12.0 | $A_{yy}$ | −0.0384 | 4.4 | 12 | ±0.0044 | ±0.0092 |
| $^{63}$Cu($\vec{d}$,$^3$He)$^{62}$Ni | 8.0 | $A_{zz}$ | −0.0401 | 6.0 | 12 | ±0.0070 | ±0.0171 |
| $^{89}$Y($\vec{d}$,$^3$He)$^{88}$Sr | 10.5 | $A_{zz}$ | −0.0394 | 1.3 | 8 | ±0.0054 | ±0.0062 |

found to be consistent with each other and were combined to yield a final $\eta_{^3\mathrm{He}}$ value of $-0.0386\pm0.0045\pm0.0012$. The first error includes statistical errors in the measurements and takes into account unknown effects which might have affected the extraction of $\eta_{^3\mathrm{He}}$. The second error is a systematic error due to the uncertainty in the beam polarization. The improvement in the present determination of $\eta_{^3\mathrm{He}}$ over previous attempts that also measured TAPs in $(d,^3\mathrm{He})$ transfer reactions is the choice of energies and targets used to improve the reliability of the DWBA calculations. Some questions still remain as to the magnitude and shape of the tensor potential which is able to fit both deuteron reaction and elastic-scattering data at energies above the Coulomb barrier. The present statistical uncertainty obtained for $\eta$ is smaller than obtained in previous determinations, however, the effects of including a different shape for the tensor potential or coupling to $(d,p)$ reaction channels provides an additional uncertainty which we are unable to estimate at this time.

The present determination of $\eta$ agrees with the results of Bhat *et al.* [19,20] who also performed a DWBA analysis to extract $\eta$, the result of Vuaridel *et al.* [17], and also Vuaridel's "world average" of $-0.037\pm0.003$. While the present result is slightly lower than the value predicted by the Los Alamos–Iowa group [5] ($-0.043\pm0.001$), it agrees with the Sendai group [6] calculation ($-0.0414\pm0.0004$). These results are summarized in Fig. 6.

A recent attempt by this group to determine $\eta$ for the triton ($\eta_t$) yielded $\eta_t=-0.0411\pm0.0013\pm0.0012$ [4]. If a ratio of $\eta_t/\eta_{^3\mathrm{He}}$ is calculated, we obtain $\eta_t/\eta_{^3\mathrm{He}}=1.06\pm0.129$ in excellent agreement with the results of the Los Alamos–Iowa ($1.06\pm0.034$) and Sendai ($1.06\pm0.014$) groups. The results of this work provide information for further tests of modern three-body calculations.

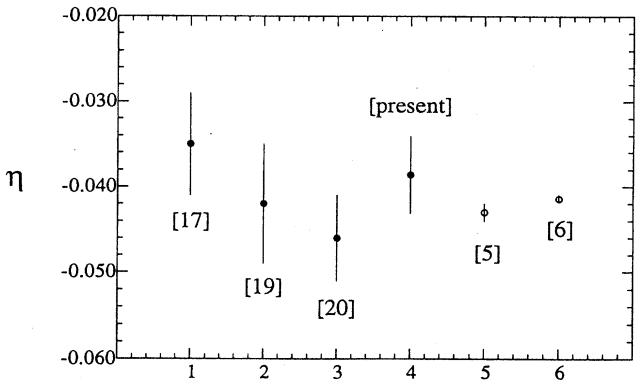


FIG. 6. Summary of recent experimental determinations and theoretical calculations of $\eta$. The solid circles are the experimental results obtained by Vuaridel *et al.* [17] and the results of Bhat *et al.* [19,20]. The open circles are the theoretical calculations with Ref. [5], the Los Alamos–Iowa group calculation and Ref. [6], the Sendai group calculation.

## ACKNOWLEDGMENTS

This work was supported by the U.S. Department of Energy through Grant No. DE-FG05-88ER40442. The authors would like to thank Dr. E. R. Crosson, Dr. K. A. Fletcher, Dr. T. C. Black, and Dr. J. C. Blackmon, and L. Ma for their help in data acquisition.

[1] A. M. Eiro and F. D. Santos, J. Phys. G **16**, 1139 (1990).
[2] T. E. O. Ericson and M. Rosa-Clot, Annu. Rev. Nucl. Sci. **35**, 271 (1985).
[3] J. L. Friar, B. F. Gibson, G. L. Payne, A. M. Bernstein, and T. E. Chupp, Phys. Rev. C **42**, 2310 (1990).
[4] B. Kozlowska, Z. Ayer, R. K. Das, H. J. Karwowski, and E. J. Ludwig, Phys. Rev. C **50**, 2695 (1994).
[5] J. L. Friar, B. F. Gibson, D. R. Lehman, and G. L. Payne, Phys. Rev. C **37**, 2859 (1988).
[6] Y. Wu, S. Ishikawa, and T. Sasakawa, Few-Body Syst. **15**, 145 (1993).
[7] M. E. Brandan and W. Haeberli, Nucl. Phys. **A287**, 213 (1977).
[8] S. Roman, A. K. Basak, J. B. A. England, J. M. Nelson, N. E. Sanderson, F. D. Santos, and A. M. Eiro, Nucl. Phys. **A289**, 269 (1977).
[9] J. A. Bieszk and L. D. Knutson, Nucl. Phys. **A349**, 445 (1980).
[10] R. C. Johnson and F. D. Santos, Part. Nucl. **2**, 285 (1971).
[11] A. A. Ioannides, M. A. Nagarajan, and R. Shyam, Phys. Lett. **103B**, 187 (1981).
[12] O. Karban and J. A. Tostevin, Phys. Lett. **103B**, 259 (1981).
[13] F. Entezami, J. D. Brown, J. M. Barnwell, K. S. Dhuga, O. Karban, J. M. Nelson, and S. Roman, Nucl. Phys. **A405**, 69 (1983).
[14] F. Merz, H. Clement, F. J. Eckle, G. Eckle, A. M. Eiro, G. Graw, H. Kader, S. Roman, P. Schiemenz, and N. Seichert, Phys. Lett. B **183**, 144 (1987).
[15] P. W. Keaton and D. D. Armstrong, Phys. Rev. C **8**, 1692 (1973).
[16] M. C. Vetterli, J. A. Kuehner, A. J. Trudel, C. L. Woods, R. Dymarz, A. A. Pilt, and H. R. Weller, Phys. Rev. Lett. **54**, 1129 (1985).
[17] B. Vuaridel, W. Gruebler, V. Konig, K. Elsener, P. S. Schmelzbach, M. Bittcher, D. Singhy, I. Borbely, M. Bruno, F. Cannata, and M. D'Agostino, Nucl. Phys. **A499**, 429 (1989).
[18] J. T. Londergan, J. C. Price, and E. J. Stephenson, Phys. Rev. C **35**, 902 (1987).
[19] C. M. Bhat, J. E. Bowsher, T. B. Clegg, H. J. Karwowski, and E. J. Ludwig, Phys. Rev. C **38**, 1537 (1988).
[20] C. M. Bhat, E. J. Ludwig, T. B. Clegg, and H. J. Karwowski, Nucl. Phys. **A526**, 36 (1991).
[21] T. B. Clegg *et al.*, Nucl. Instrum. Methods Phys. Res. Sect. A **357**, 200 (1995).
[22] S. A. Tonsfeldt, Ph.D. dissertation, University of North Carolina at Chapel Hill, 1980, available from University Microfilms International, 300 N. Zeeb Road, Ann Arbor, MI 48106, Order No. 8022515.
[23] M. H. Macfarlane and S. C. Pieper, Argonne National Laboratory Report No. ANL-76-11, Rev. 1 (unpublished), modified by R. P. Goddard (1980).

[24] W. W. Daehnick, J. D. Childs, and Z. Vrcelj, Phys. Rev. C **21**, 2253 (1980). Potential $L$ from Table III was used.
[25] J. M. Lohr and W. Haeberli, Nucl. Phys. **A232**, 381 (1974). Potential parameters defined by Eqs. (1)–(3) were used, with $a_0$=0.86 fm.
[26] G. Perrin, Nguyen Van Sen, J. Arvieux, R. Darves-Blanc, J. L. Durand, A. Fiore, J. C. Gondrand, F. Merchez, and C. Perrin, Nucl. Phys. **A282**, 221 (1977). Potential parameters of Table IV were used.
[27] F. D. Becchetti and G. W. Greenlees, *Polarization Phenomena in Nuclear Reactions* (University of Wisconsin Press, Madison, 1971), p. 682.
[28] R. P. Goddard and W. Haeberli, Nucl. Phys. **A316**, 116 (1979).
[29] J. Cook, Comp. Phys. Commun. **31**, 363 (1984).
[30] R. Frick, H. Clement, G. Graw, P. Schiemenz, N. Seichert, and Sun Tsu-Hsun, Z. Phys. A **319**, 133 (1984).
[31] J. E. Kammeraad and L. D. Knutson, Nucl. Phys. **A435**, 502 (1985).
[32] N. L. Rodning and L. D. Knutson, Phys. Rev. C **41**, 898 (1990).
[33] L. D. Knutson and W. Haeberli, Phys. Rev. C **12**, 1469 (1975).
[34] F. D. Santos, Z. Phys. **A295**, 73 (1980).
[35] J. A. Tostevin, Nucl. Phys. **A466**, 349 (1987).
[36] B. C. Karp, E. J. Ludwig, J. E. Bowsher, B. L. Burks, and T. B. Clegg, Nucl. Phys. **A457**, 15 (1986).
[37] A. H. Rosenfeld, Annu. Rev. Nucl. Sci. **25**, 555 (1975).